OPEN ACCESS
International Journal of Innovations in Science & Technology

Design of Microgrid Using Floating PV, Hydro, And Wind for Power Generation and Quality Output Power at Takht Bhai, Mardan

Bheeraj Kumar, Aaima Waqar, Izaz Ali Shah, Muhammad Awais, Bilal Ur Rehman, Muhammad Iftikhar Khan and Muhammad Amir

Department of Electrical Engineering, Faculty of Electrical and Computer Engineering, University of Engineering and Technology, Peshawar, Pakistan

*Correspondence: bur@uetpeshawar.edu.pk

Citation | Kumar. B, Waqar. A, Shah. I. A, Awais. M, Rehman. B. U, Khan. M. I, Amir. M, "Design of Microgrid Using Floating PV, Hydro, And Wind for Power Generation and Quality Output Power at Takht Bhai, Mardan", IJIST, Vol. 8 Issue. 3 pp 1207-1227, June 2026

Received | April 20, 2026 **Revised |** May 23, 2026 **Accepted |** May 30, 2026 **Published |** June 12, 2026.

This research presents the design and simulation of a hybrid microgrid system for the Takht Bhai region of Mardan, Pakistan, integrating floating photovoltaic (FPV), small-scale hydro, and wind energy resources. The proposed system was modeled in DIgSILENT PowerFactory using a 38-bus distribution network to evaluate load flow, voltage stability, short-circuit performance, and power quality. Simulation results showed that the voltage at the point of common coupling remained stable at approximately 1.06 p.u. under normal operating conditions. During a 50 ms short-circuit event, the POC_BUS voltage dropped to 0 p.u. and recovered immediately to 1.06 p.u. after fault clearance, indicating strong fault ride-through capability. The 132 kV POC_BUS recorded a three-phase maximum short-circuit current of 14.09 kA and a peak current of 34.77 kA, while the minimum three-phase fault current was 12.07 kA. At the 0.4 kV inverter bus level, three-phase maximum fault currents ranged from 3.46 to 3.81 kA, whereas the 33 kV collection level showed fault currents of up to 51.75 kA. Power quality assessment based on the P28 Engineering Recommendation confirmed acceptable voltage fluctuation and flicker performance. The results demonstrate that the coordinated use of hydro, FPV, and wind resources improves voltage regulation, enhances system reliability, and provides a technically feasible renewable energy solution for rural electrification.

Keywords: FPV, HMG, Wind Energy, Power Factory, Small-Scale Hydro.

Introduction:

Electricity reliability remains a major challenge in Pakistan, particularly in rural and semi-urban areas where load shedding, voltage instability, and dependence on fossil-fuel-based generation affect social and economic development [1]. Microgrids have emerged as an effective decentralized energy solution because they can integrate local distributed energy resources and operate in both grid-connected and islanded modes [2]. Recent studies show that renewable-energy-based hybrid microgrids can improve energy access, reduce fuel dependency, and support sustainable rural electrification [3].

Floating photovoltaic (FPV) technology is gaining increasing attention because it utilizes water surfaces for solar generation, reduces land occupation, decreases water evaporation, and improves PV efficiency through natural cooling [4][5]. When FPV is combined with hydropower, the hydro resource can compensate for solar intermittency and provide dispatchable support during low irradiance periods [6]. In addition, wind energy can complement solar generation because wind availability often differs from solar production patterns, improving the continuity of renewable power supply [7].

However, renewable-energy-integrated microgrids face technical challenges such as voltage fluctuation, frequency instability, fault-current variation, harmonics, and flicker [8]. These challenges require detailed load-flow studies, short-circuit analysis, power quality assessment, reactive power compensation, and dynamic stability evaluation [9][10]. Therefore, this study designs and analyzes a hybrid microgrid integrating floating PV, small hydro, and wind energy for Takht Bhai, Mardan using DIgSILENT PowerFactory. The study evaluates voltage stability, fault behavior, and power quality performance to support reliable renewable-based rural electrification.

Problem Statement:

Pakistan continues to face serious energy shortages, especially in rural areas where people often struggle with unreliable electricity. At the same time, the country depends heavily on fossil fuels, which are expensive and harmful to the environment. The area around Takht Bhai, District Mardan, has natural resources such as flowing canals, extensive water bodies, and favourable wind conditions, but these are not being used effectively for clean power generation. The natural resources are intermittent and variable, which creates power quality issues such as voltage fluctuations, frequency instability, and harmonics.

Novelty of the Study:

The proposed research presents a novel hybrid renewable microgrid framework integrating Floating Photovoltaic (FPV), small hydro, and wind energy resources for the Takht Bhai region in Mardan, Pakistan. Although previous studies have investigated individual renewable systems or limited hybrid combinations, very few studies have comprehensively integrated FPV, hydro, and wind resources within a unified distribution-level microgrid while simultaneously evaluating voltage stability, short-circuit behavior, and power quality performance under realistic operating conditions.

The primary novelty of this work lies in the development of a 38-bus hybrid renewable microgrid model using DIgSILENT PowerFactory based on site-specific renewable resource assessment for the Takht Bhai region. Unlike conventional studies that mainly focus on economic analysis or energy generation estimation, the proposed study performs detailed load flow analysis, fault current analysis according to IEC 60909 standards, dynamic voltage recovery assessment, and P28-based power quality evaluation.

Another important contribution is the integration of Static Var Compensator (SVC)-based reactive power support to improve voltage regulation and mitigate flicker effects caused by renewable energy intermittency. The study also evaluates the fault ride-through capability of the hybrid microgrid during transient disturbances, demonstrating rapid voltage recovery and stable post-fault operation at the point of common coupling.

Furthermore, the use of floating photovoltaic technology over existing canal water surfaces introduces an efficient approach for reducing land utilization issues while improving solar panel efficiency through natural water cooling. Therefore, the proposed work contributes a technically comprehensive and region-specific renewable microgrid solution for rural electrification, combining renewable resource integration, power quality enhancement, and system stability analysis within a single framework.

Aims and objectives:

The main aim of this research is to design and evaluate a hybrid renewable microgrid integrating Floating Photovoltaic (FPV), small hydro, and wind energy resources for the Takht Bhai region in Mardan, Pakistan, in order to improve voltage stability, power quality, and system reliability using renewable energy sources.

The objectives of the study are as follows:

To develop a 38-bus hybrid renewable microgrid model using DIgSILENT PowerFactory based on site-specific renewable resource data.

To evaluate the voltage profile and power flow performance of the proposed microgrid under normal operating conditions.

To analyze short-circuit current levels and fault ride-through capability under different fault scenarios.

To assess voltage stability and power quality performance according to P28 standards.

To investigate the effectiveness of SVC-based reactive power compensation for improving voltage regulation and reducing flicker effects.

To validate the technical feasibility of the proposed hybrid renewable microgrid for sustainable rural electrification in Pakistan.

Scope of research work:

Renewable energy sources such as solar and wind are rapidly growing due to increasing awareness of fossil fuel depletion and environmental concerns. This shift has made hybrid microgrids an effective solution for providing reliable and sustainable electricity, especially in rural areas facing power shortages. This project focuses on designing a hybrid microgrid for the Takht Bhai area by integrating floating solar, small hydro, and wind energy. The system will be modeled and simulated to ensure stable voltage, consistent frequency, and good power quality. The work includes studying microgrid technologies, analyzing hybrid system components, and properly sizing them for efficient operation. The design and simulation will be carried out using DIgSILENT PowerFactory, along with considering appropriate operational strategies to enhance system performance to enhance system performance. The main motivation is to develop a clean, reliable, and cost-effective energy solution using local resources, which can also serve as a model for other rural areas in Pakistan.

Statement of the Work:

The data used for the proposed work were collected and processed in MS Excel, and the model was designed, analysed, and simulated in PowerFactory (Software). Initially, data on solar irradiance, wind speed, water flow, and load demand for the Takht Bhai area were collected and analysed to assess the available renewable energy potential and electricity requirements. In the next step, different load profiles for the microgrid were generated using standard load modelling techniques, and the hybrid microgrid system was designed and sized by integrating floating solar, small hydro, and wind energy sources. The system model was then developed and simulated using DIgSILENT PowerFactory. After that, system performance was evaluated by analysing key parameters, including voltage stability, frequency behaviour, and overall power quality, under different operating conditions. Optimisation techniques and an energy management approach were considered to improve the efficient utilisation of available resources. Finally, the microgrid was tested under different operating scenarios to assess its reliability and performance, and the results were used to conclude the study and suggest an effective hybrid energy solution for rural electrification.

Literature Review:

Hybrid renewable energy systems have been widely studied as practical solutions for reducing fossil fuel dependency and improving energy reliability in remote communities. Solar, wind, hydro hybrid systems are especially effective because each resource has different generation characteristics, allowing one source to compensate for another during resource variability [11]. Recent optimization studies confirm that hybrid renewable energy systems can reduce energy cost and improve supply reliability when properly sized and controlled [12].

FPV systems have become an important research area due to their ability to improve solar energy production while reducing land-use conflicts. Studies on hybrid FPV plant designs show that FPV can be effectively combined with hydropower, pumped storage, hydrogen production, and other renewable systems [5]. Global assessments of FPV, hydropower systems demonstrate that combining solar and hydro resources increases energy flexibility and improves utilization of existing hydropower infrastructure [4]. Recent FPV reviews also highlight improved thermal performance, reduced evaporation, and better land conservation compared with conventional ground-mounted PV systems [13].

Wind energy integration is also important in hybrid renewable microgrids. Wind–solar systems provide complementary generation patterns and can reduce renewable intermittency when supported by suitable control and storage technologies [14]. However, high penetration of wind and solar resources can create voltage instability, harmonics, flicker, and frequency regulation problems [15]. Therefore, power-electronic converter control, reactive power support, and coordinated energy management are essential for maintaining microgrid stability [16].

Microgrid stability has been extensively studied in recent literature. Stability problems are commonly classified into small-signal stability, transient stability, voltage stability, and frequency stability [8]. Advanced inverter control strategies, hierarchical control, droop control, and virtual synchronous generator techniques have been proposed to improve renewable microgrid performance [17][18]. Reactive power compensation devices such as SVCs and STATCOMs are also widely used to improve voltage regulation and power quality in renewable-integrated networks [19].

Energy storage systems play a key role in hybrid microgrids by smoothing renewable power fluctuations, supporting frequency regulation, and improving fault ride-through performance [9]. Battery storage, supercapacitors, flywheels, and pumped hydro storage have been widely investigated for microgrid applications [20]. Recent studies show that properly sized storage improves operational reliability and reduces renewable curtailment [21].

Recent research further emphasizes techno-economic optimization, reliability assessment, and real-time energy management in hybrid renewable microgrids [22]. Optimization methods such as mixed-integer linear programming, particle swarm optimization, and artificial intelligence-based control have been applied to improve component sizing and operational scheduling [23]. Recent studies also show that renewable microgrids can support sustainable development by improving energy access, reducing emissions, and strengthening local energy resilience [24].

Despite these developments, limited research has jointly evaluated FPV, hydro, and wind integration in a realistic distribution-level microgrid while simultaneously considering load flow, short-circuit analysis, voltage recovery, and power quality compliance. Therefore, the present study addresses this gap by developing a 38-bus hybrid microgrid model for Takht Bhai, Mardan and analyzing its technical performance using Dig SILENT Power Factory [25][26].

Methodology:

Figure 1 presents the complete workflow adopted for the design, simulation, and performance evaluation of the proposed hybrid renewable microgrid for Takht Bhai, Mardan. Each stage of the methodology is explained step by step as follows.

First, the project location was selected at Takht Bhai, District Mardan, due to the availability of renewable energy resources, including canal water flow, open water surfaces suitable for floating photovoltaic installation, and favorable wind conditions. The site was considered suitable for developing a hybrid microgrid for rural electrification.

Second, resource assessment was performed by collecting and analyzing hydrological, solar irradiance, wind speed, climatic, and load demand data for the selected region. Hydrological data were used to estimate the small hydro generation potential, solar irradiance data were used for FPV sizing, wind speed data were used to evaluate wind turbine output, and load demand data were used to define the electrical requirements of the proposed microgrid.

Third, hybrid microgrid planning was carried out by integrating three renewable energy resources: small hydro, floating PV, and wind generation. The purpose of this stage was to develop a balanced renewable energy system in which hydro generation provides a stable base supply, while FPV and wind generation support the load according to resource availability.

Fourth, the complete system was modeled in DIgSILENT PowerFactory. The software environment was used to develop the electrical network, assign equipment ratings, configure generation units, and simulate different operating scenarios. The modeling process ensured that the proposed microgrid represented practical distribution-level operating conditions.

Fifth, a 38-bus network was designed to represent the hybrid microgrid connection structure. The network included low-voltage inverter buses, transformer buses, 33 kV collection buses, generator buses, and the 132 kV point of common coupling. This structure allowed detailed evaluation of voltage profiles, power flow, and fault levels at different voltage levels.

Sixth, component configuration was performed by defining the slack bus, hydro generator, floating PV inverters, wind generator, transformers, loads, and auxiliary buses. The external utility grid was assigned as the slack bus to maintain power balance, while renewable generation units were configured according to their operating characteristics.

Seventh, load-flow analysis was carried out to evaluate the steady-state performance of the proposed microgrid. This analysis was used to determine bus voltages, line loading, active and reactive power flow, and network losses under normal operating conditions.

Eighth, short-circuit analysis was performed according to IEC 60909 standards. Different fault scenarios, including three-phase maximum, single-phase maximum, three-phase minimum, and single-phase minimum faults, were analyzed at various buses. The calculated fault currents were used to assess equipment rating requirements and protection coordination.

Ninth, power quality analysis was conducted according to Engineering Recommendation P28. Flicker severity indices and voltage fluctuation behavior were evaluated to determine whether the proposed microgrid satisfied acceptable power quality limits.

Tenth, an SVC was integrated into the system to provide dynamic reactive power compensation. The SVC was used to improve voltage regulation, reduce voltage fluctuation, and mitigate flicker effects caused by renewable energy intermittency.

Finally, the overall performance of the proposed microgrid was evaluated through voltage profile analysis, power-flow assessment, network loss evaluation, short-circuit current assessment, fault ride-through behavior, and P28 compliance verification. The results obtained from these analyses were used to validate the technical feasibility and reliability of the proposed hybrid microgrid for rural electrification.

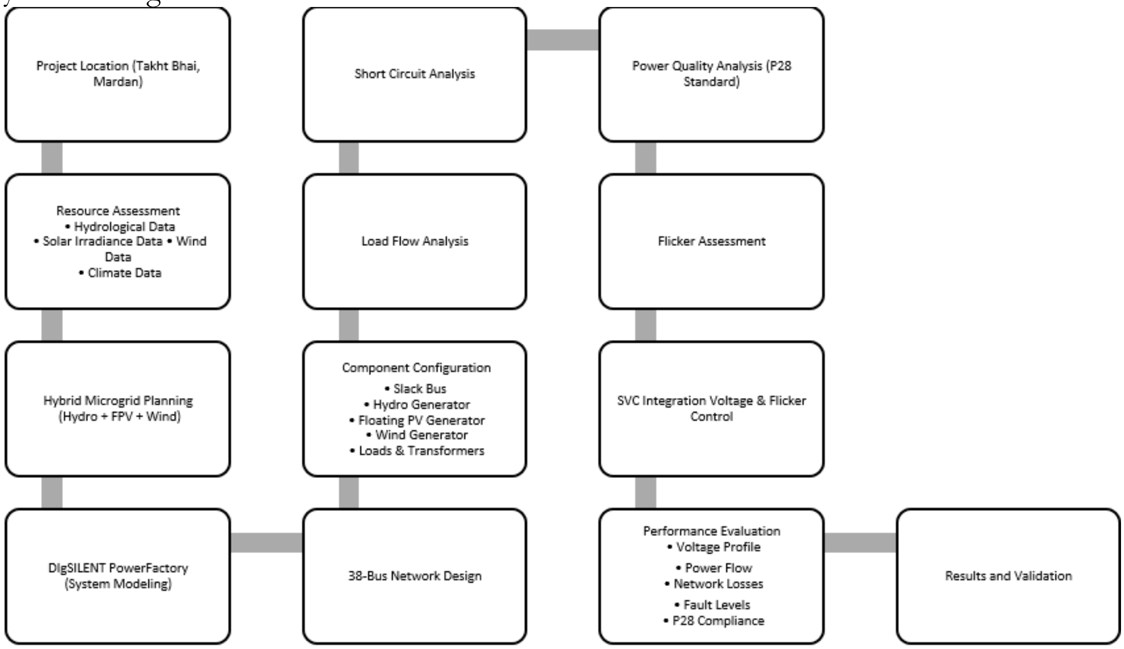

Figure 1. Flowchart.

Justification of 38-Bus Network and Simulation Assumptions:

The 38-bus network was selected because it provides a detailed representation of the proposed hybrid microgrid architecture for the Takht Bhai region. The network includes low-voltage inverter buses for FPV generation, transformer low-voltage and high-voltage buses, 33 kV collection buses, generator buses, auxiliary buses, and the 132 kV point of common coupling with the utility grid. This configuration allows the system to represent the practical interconnection of floating PV, small hydro, wind generation, step-up transformers, local loads, and grid interface within one simulation model.

The 38-bus structure was also chosen to enable detailed technical analysis at different voltage levels. The 0.4 kV buses represent inverter-side renewable generation, the 11 kV and 33 kV buses represent generator and collection network levels, and the 132 kV bus represents the grid connection point. Therefore, the selected network size is sufficient to evaluate voltage profiles, power-flow distribution, short-circuit current levels, and power quality behavior throughout the proposed hybrid microgrid.

The DIgSILENT PowerFactory model was developed using the following simulation assumptions. The external utility grid was modeled as the slack bus to maintain system voltage and active/reactive power balance. Renewable generation units were assumed to operate under available resource conditions obtained from solar irradiance, wind speed, and hydrological data. The floating PV system was modeled as inverter-based generation connected to 0.4 kV buses through step-up transformers. The hydro generator was modeled as a synchronous generator connected to the medium-voltage network. The wind generation unit was connected through appropriate converter and transformer interfaces.

Load-flow analysis was performed under steady-state operating conditions to evaluate voltage magnitude, power-flow distribution, and network losses. Short-circuit analysis was carried out according to IEC 60909 standards using maximum and minimum fault current conditions. Four fault cases were considered: three-phase maximum, single-phase maximum, three-phase minimum, and single-phase minimum faults. Dynamic RMS simulation was performed for a 5-second time window, where a fault was applied at 0.45 s and cleared at 0.50 s to evaluate voltage recovery and fault ride-through performance.

Power quality assessment was conducted according to Engineering Recommendation P28. Flicker severity and voltage fluctuation behavior were evaluated at the point of common coupling. A Static Var Compensator was included in the simulation model to provide dynamic reactive power support, improve voltage regulation, and reduce flicker effects. These assumptions and parameters were selected to ensure that the simulation model realistically represents the operating behavior of the proposed hybrid renewable microgrid.

Materials and Methods:

The proposed hybrid renewable microgrid was developed for the Takht Bhai region in District Mardan, Pakistan, using Floating Photovoltaic (FPV), small hydro, and wind energy resources. The complete system was modeled and simulated in DIgSILENT PowerFactory using a 38-bus distribution network for load flow, short-circuit, voltage stability, and power quality analysis.

Renewable Resource Assessment:

The renewable resource assessment was carried out using regional climatic and electrical load data. Solar irradiance data for the Takht Bhai region were analyzed to estimate the available solar energy potential for floating photovoltaic generation. Wind speed data were evaluated to determine the operational suitability and expected power generation of wind turbines. Hydrological data, including canal water flow rate and available head, were used to estimate small hydroelectric generation capacity. Load demand data for the selected region were also analyzed to determine the required generation capacity and network loading conditions.

Hybrid Microgrid Configuration:

The proposed microgrid consisted of three major renewable generation sources:

Floating photovoltaic generation system connected through inverter-based low-voltage buses.

Small hydro generation unit connected through generator transformers to the medium-voltage network.

Wind generation unit integrated into the distribution network for supplementary renewable generation.

The microgrid included low-voltage 0.4 kV inverter buses, 33 kV collection buses, and a 132 kV point of common coupling connected to the utility grid. The external utility grid was configured as the slack bus for maintaining active and reactive power balance during simulations.

Component Ratings and Network Design:

The system was modeled using a 38-bus network structure. The main electrical components and ratings used in the proposed system are summarized below:

Inverter buses: 0.4 kV rated voltage.

Auxiliary low-voltage bus: 0.415 kV.

Medium-voltage collection buses: 33 kV rated voltage.

Generator low-voltage side: 11 kV.

Point of common coupling (POC_BUS): 132 kV rated voltage.

Floating PV inverter buses operated at approximately 1.11 p.u. voltage magnitude during steady-state operation.

POC_BUS operated at approximately 1.06 p.u. under normal operating conditions.

Transformers were configured to connect renewable generation sources to the medium-voltage network, while the utility grid connection was established through grid transformers connected to the 132 kV network.

Load Flow and Voltage Stability Analysis:

Load-flow analysis was performed using DIgSILENT PowerFactory to evaluate steady-state network performance. The analysis included voltage profile assessment, active and reactive power flow calculation, and network loss evaluation under normal operating conditions. Bus voltages were monitored throughout the network to verify that voltage magnitudes remained within acceptable operating limits.

Short-Circuit Analysis:

Short-circuit analysis was carried out according to IEC 60909 standards. Four fault scenarios were analyzed at different buses of the network:

Three-phase maximum fault.

Single-phase maximum fault.

Three-phase minimum fault.

Single-phase minimum fault.

The initial symmetrical short-circuit current (Ik) and peak short-circuit current (Ip) were calculated for each fault condition. These values were used to evaluate equipment rating requirements, protection coordination, and fault withstand capability of the proposed microgrid.

Dynamic Voltage Recovery and Fault Ride-Through Analysis:

Dynamic simulations were performed to evaluate voltage recovery behavior during transient fault conditions. A line-to-line fault was applied at the point of common coupling at t = 0.45 s and cleared at t = 0.50 s. The voltage response at POC_BUS was monitored to evaluate the fault ride-through capability and post-fault voltage recovery performance of the hybrid microgrid.

Power Quality Assessment:

Power quality analysis was performed according to Engineering Recommendation P28 standards. Voltage fluctuation and flicker severity indices were evaluated to determine the impact of renewable energy intermittency on network performance. The results were used to assess the overall power quality compliance of the proposed microgrid.

Reactive Power Compensation and Optimization:

A Static Var Compensator (SVC) was integrated into the network to provide dynamic reactive power support. The SVC was used to improve voltage regulation, reduce voltage fluctuation, and mitigate flicker effects caused by renewable generation variability. The operational coordination between FPV, hydro, and wind resources was also evaluated to improve overall system stability and renewable energy utilization efficiency.

Performance Validation:

The final performance of the proposed hybrid microgrid was validated using voltage profile analysis, short-circuit current evaluation, power-flow assessment, network loss analysis, and power quality verification. The simulation results were used to confirm the technical feasibility and operational reliability of the proposed renewable microgrid for rural electrification applications.

Simulation Results and Analysis:

Short circuit analysis is performed in DIgSILENT Power Factory as shown in Figure 2 to determine the fault currents that flow in the Takht Bhai microgrid network when a short circuit occurs at any point in the system. The results are used to verify that circuit breakers and protective relays are correctly rated and coordinated. The analysis follows the IEC 60909:2016 standard and covers four fault scenarios at every bus: three-phase maximum, single-phase maximum, three-phase minimum, and single-phase minimum. Also, a Table 1 is provided for the Bus Voltages obtained using simulation tool.

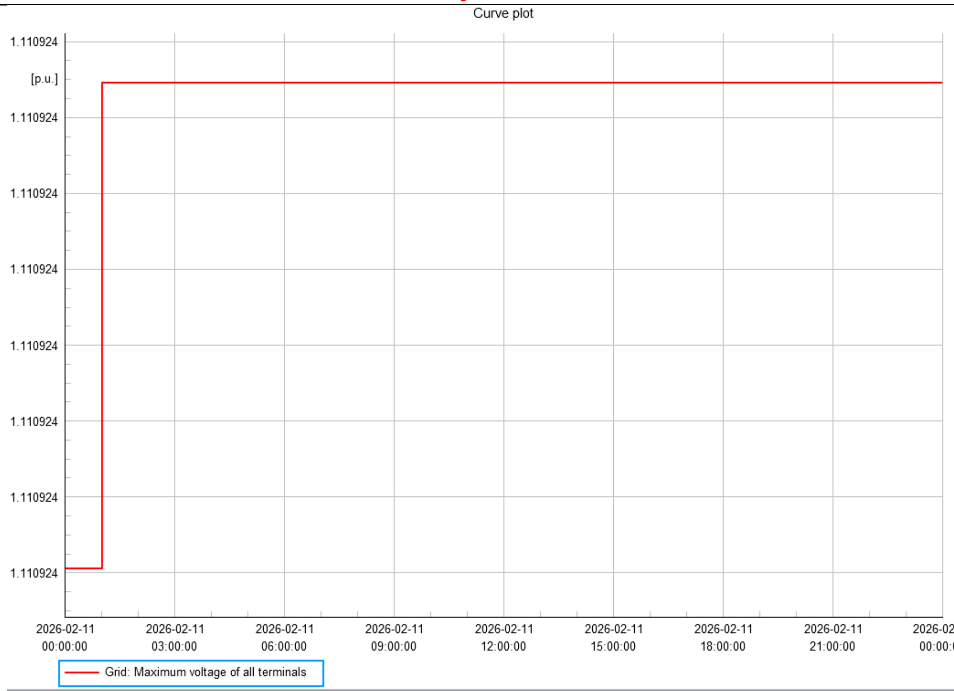

Figure 2. Bus Voltages

Table 1. Bus voltages

Name	GRID	L-L voltage (KV)	Magnitude L-L Voltage (KV)	L-L Voltage in (p.u)	L-G voltages
Inv_TF_LV_01	GRID	0.4	0.44	1.099	0.25390763
Inv_TF_LV_02	GRID	0.4	0.44	1.099	0.25390763
Inv_TF_LV_03	GRID	0.4	0.44	1.099	0.25390763
Inv_bus_01	GRID	0.4	0.444	1.111	0.25655681
Inv_bus_02	GRID	0.4	0.444	1.111	0.25655681
Inv_bus_03	GRID	0.4	0.444	1.111	0.25655681
Inv_bus_04	GRID	0.4	0.444	1.111	0.25655681
Inv_bus_05	GRID	0.4	0.444	1.111	0.25655681
Inv_bus_06	GRID	0.4	0.444	1.111	0.25655681
Inv_bus_07	GRID	0.4	0.444	1.111	0.25655681
Inv_bus_08	GRID	0.4	0.444	1.111	0.25655681
Inv_bus_09	GRID	0.4	0.444	1.111	0.25655681
Inv_bus_10	GRID	0.4	0.444	1.111	0.25655681
Inv_bus_11	GRID	0.4	0.444	1.111	0.25655681
Inv_bus_12	GRID	0.4	0.444	1.111	0.25655681
Inv_bus_13	GRID	0.4	0.444	1.111	0.25655681
Inv_bus_14	GRID	0.4	0.444	1.111	0.25655681
Inv_bus_15	GRID	0.4	0.444	1.111	0.25655681
Inv_bus_16	GRID	0.4	0.444	1.111	0.25655681
Inv_bus_17	GRID	0.4	0.444	1.111	0.25655681
Inv_bus_18	GRID	0.4	0.444	1.111	0.25655681
Inv_bus_19	GRID	0.4	0.444	1.111	0.25655681
Inv_bus_20	GRID	0.4	0.444	1.111	0.25655681
Inv_bus_21	GRID	0.4	0.444	1.111	0.25655681
Inv_bus_22	GRID	0.4	0.444	1.111	0.25655681
Inv_bus_23	GRID	0.4	0.444	1.111	0.25655681

Inv_bus_24	GRID	0.4	0.444	1.111	0.25655681
Aux LV	GRID	0.415	0.439	1.057	0.25318087
Gen LV	GRID	11	12.215	1.11	7.05230897
GT_LV side	GRID	33	35.631	1.08	20.5714758
Aux HV	GRID	33	35.648	1.08	20.5812328
33kV switchboard	GRID	33	35.648	1.08	20.5812575
Inv_TF_HV_01	GRID	33	35.65	1.08	20.5825627
Inv_TF_HV_02	GRID	33	35.65	1.08	20.5825627
Inv_TF_HV_03	GRID	33	35.65	1.08	20.5825627
Gen HV	GRID	33	35.65	1.08	20.5826947
POC_BUS	GRID	132	139.92	1.06	80.7828453
GT_HV side	GRID	132	139.923	1.06	80.7844196

For each scenario, two current values are calculated: the initial symmetrical short circuit current Ik (kA), which is the RMS value of the AC component of the fault current at the instant of fault inception, and the peak short circuit current Ip (kA), which is the maximum instantaneous current including the DC offset. The Ik value is used for thermal rating of equipment, while Ip is used for the mechanical withstand rating of busbars and circuit breakers.

A time-domain RMS simulation is carried out in DIgSILENT PowerFactory to observe the voltage behavior at the point of connection bus (POC_BUS) during a line-to-line short circuit event. The simulation runs from t = 0 s to t = 5 s. A three-phase bolted fault is applied at t = 0.45 s and cleared at t = 0.50 s, representing a 50 ms fault duration consistent with 132 kV protection operating times. The POC_BUS voltage magnitude per unit is recorded throughout the simulation and is presented in Figure 3.

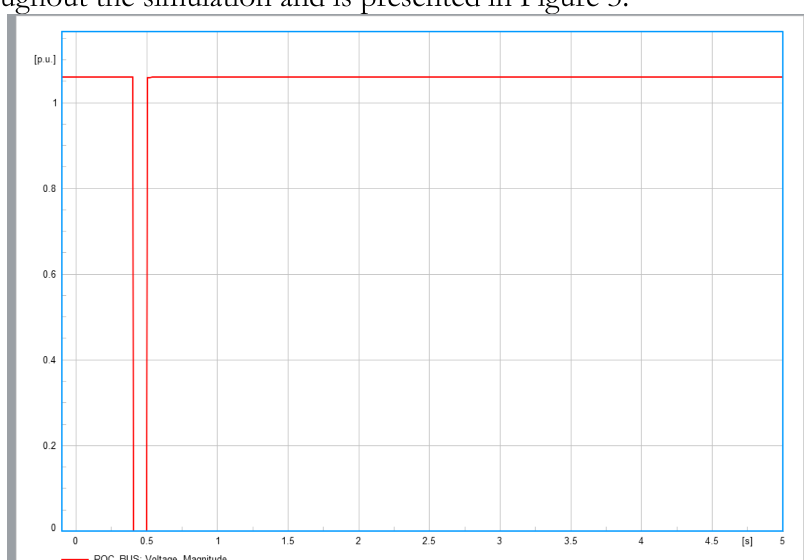

Figure 3. Voltage Response at POC_BUS During Line-to-Line Fault

The voltage at POC_BUS is plotted in three different phases. Prior to the fault (t = 0 to 0.45 s) the bus voltage remains constant at around 1.06 p.u. (139.92 kV on the 132 kV nominal base). This is the typical pre fault voltage of the lightly loaded and slightly overloaded voltage-controlled PESCO 132 kV network in Mardan.

The bolted line-to-line fault is applied to POC_BUS at t = 0.45 s. The voltage drops to 0.0 p.u. instantly and stays at zero values during the fault period of 50ms. The voltage collapsing to nominal zero demonstrates that the simulation correctly represents a bolted fault with no fault impedance. Hence, results in the maximum fault current contribution from the PESCO grid and all local generators.

Once the fault is cleared by the protection system at t = 0.50 s, the behaviour of the POC_BUS voltage recovers fully and instantaneously to its pre fault value of 1.06 p.u. with no transient oscillation or sustained undervoltage following the fault. This clean recovery, which is a time of 50 milliseconds, is a good representation of the synchronous hydro generator maintaining its excitation and internal voltage during the fault period and resynchronising immediately as soon as the fault is cleared. The behaviour shows the microgrid has the necessary fault ride through capability at the 132 kV connection point. Further, Table 2 is provided for POC Bus voltages during the short circuit.

Table 2. POC_BUS voltage behavior during the short circuit event

Phase of Event	Time (s)	Voltage (p.u.)	Voltage (kV)	Observation
Prefault	0 to 0.45	1.060	139.92	Normal operating voltage, stable
Fault applied	t = 0.45	0.000	0.00	Instantaneous collapse to zero
Fault duration	0.45 to 0.50	0.000	0.00	50 ms fault clearing period
Post-fault recovery	t > 0.50	1.060	139.92	Full recovery, no oscillation

The short circuit currents for each bus are provided in the following manner: four fault conditions are considered (three-phase maximum, single-phase maximum, three-phase minimum and single-phase minimum), and for each fault condition, the initial symmetrical short circuit current (Ik) and the peak short circuit current (Ip) are provided in kA. Equipment ratings will utilize the maximum values, while relay sensitivity verification will employ the minimum values. The repeated current values observed in Table 3 indicate that several buses within the proposed hybrid microgrid experience similar fault current magnitudes due to their electrical proximity, common voltage levels, and equivalent network impedance characteristics. These repeated values are mainly associated with buses connected through identical transformer configurations and short electrical distances within the 33 kV collection network.

From an engineering perspective, the observed fault current distribution provides important information regarding network strength and protection system coordination. Similar current magnitudes at neighboring buses indicate balanced power distribution and consistent impedance characteristics within the renewable generation collection system. This behavior confirms that the proposed network configuration maintains stable electrical coupling between floating photovoltaic, hydro, and wind generation units.

The fault current values also have direct implications for the selection and sizing of protection equipment such as circuit breakers, relays, transformers, and switchgear components. Higher short-circuit current levels at the 33 kV buses indicate that medium-voltage protection devices must possess adequate fault withstand capability to safely interrupt fault currents during abnormal operating conditions.

In contrast, the lower fault current values observed at inverter-connected low-voltage buses reflect the limited fault current contribution characteristics of inverter-based renewable energy systems. Unlike synchronous generators, inverter-based systems typically contribute lower short-circuit currents due to converter control limitations. This characteristic is important for modern renewable-integrated protection system design and fault detection strategies.

The repeated current values therefore confirm the electrical consistency of the proposed 38-bus network and demonstrate that the hybrid renewable microgrid operates within acceptable protection and fault withstand limits. These results further support the technical feasibility and operational reliability of the proposed FPV–hydro–wind hybrid microgrid under fault conditions.

Table 3. Short circuit current results for all buses

IK(KA)	IP(KA)	IK(KA)	IP(KA)	IK(KA)	IP(KA)	IK(KA)	IP(KA)
3.7674	8.6665	2.8016	1.2179	3.3319	7.6153	2.5106	1.0984
3.7632	8.6474	2.7968	1.2171	3.3280	7.5932	2.5046	1.0977
6.1797	13.2866	13.3802	6.2232	5.3890	11.5848	11.6675	5.4275
13.9278	34.2459	34.3530	13.9713	11.9316	29.2158	29.3613	11.9910
3.8078	8.8263	2.8138	1.2139	3.3706	7.8027	2.5346	1.0949
3.7494	8.5963	2.7962	1.2196	3.3154	7.5379	2.5009	1.1000
3.4614	7.6994	7.1649	3.2211	3.1369	6.9678	6.4944	2.9238
3.7429	8.5544	2.7730	1.2133	3.3085	7.4845	2.4754	1.0942
3.7429	8.5544	2.7730	1.2133	3.3085	7.4845	2.4754	1.0942
3.7429	8.5544	2.7730	1.2133	3.3085	7.4845	2.4754	1.0942
51.7481	128.1195	131.9088	53.2787	42.9350	106.1989	112.3267	45.4124
51.7481	128.1195	131.9088	53.2787	42.9350	106.1989	112.3267	45.4124
51.7481	128.1195	131.9088	53.2787	42.9350	106.1989	112.3267	45.4124
16.6016	29.0395	16.8775	9.6487	12.5916	19.7196	11.2746	7.1992
16.6016	29.0395	16.8775	9.6487	12.5916	19.7196	11.2746	7.1992
16.6016	29.0395	16.8775	9.6487	12.5916	19.7196	11.2746	7.1992
16.6016	29.0395	16.8775	9.6487	12.5916	19.7196	11.2746	7.1992
16.6016	29.0395	16.8775	9.6487	12.5916	19.7196	11.2746	7.1992
16.6016	29.0395	16.8775	9.6487	12.5916	19.7196	11.2746	7.1992
16.6016	29.0395	16.8775	9.6487	12.5916	19.7196	11.2746	7.1992
16.6016	29.0395	16.8775	9.6487	12.5916	19.7196	11.2746	7.1992
16.6016	29.0395	16.8775	9.6487	12.5916	19.7196	11.2746	7.1992
16.6016	29.0395	16.8775	9.6487	12.5916	19.7196	11.2746	7.1992
16.6016	29.0395	16.8775	9.6487	12.5916	19.7196	11.2746	7.1992
16.6016	29.0395	16.8775	9.6487	12.5916	19.7196	11.2746	7.1992
16.6016	29.0395	16.8775	9.6487	12.5916	19.7196	11.2746	7.1992
16.6016	29.0395	16.8775	9.6487	12.5916	19.7196	11.2746	7.1992
16.6016	29.0395	16.8775	9.6487	12.5916	19.7196	11.2746	7.1992
16.6016	29.0395	16.8775	9.6487	12.5916	19.7196	11.2746	7.1992
16.6016	29.0395	16.8775	9.6487	12.5916	19.7196	11.2746	7.1992
16.6016	29.0395	16.8775	9.6487	12.5916	19.7196	11.2746	7.1992
16.6016	29.0395	16.8775	9.6487	12.5916	19.7196	11.2746	7.1992
16.6016	29.0395	16.8775	9.6487	12.5916	19.7196	11.2746	7.1992
16.6016	29.0395	16.8775	9.6487	12.5916	19.7196	11.2746	7.1992
16.6016	29.0395	16.8775	9.6487	12.5916	19.7196	11.2746	7.1992
16.6016	29.0395	16.8775	9.6487	12.5916	19.7196	11.2746	7.1992
16.6016	29.0395	16.8775	9.6487	12.5916	19.7196	11.2746	7.1992
16.6016	29.0395	16.8775	9.6487	12.5916	19.7196	11.2746	7.1992
14.0923	34.7749	35.2556	14.2871	12.0689	29.7806	30.2397	12.2549

Discussion:

Figure 4 is a clear variation in fault current levels across the three voltage tiers of the microgrid. At the 0.4 kV inverter bus level, the three-phase maximum fault current ranges from 3.46 to 3.81 kA at the inverter transformer LV buses and from 3.74 to 3.81 kA at the individual inverter buses, with corresponding peak currents of 7.70 to 8.83 kA. These values reflect the combined contribution of the floating PV inverters and the upstream grid feeding through the step-down transformers.

At the 33 kV collection level, the fault current increases significantly. The inverter transformer HV buses (Inv_TF_HV_01 to 03) show a three-phase maximum Ik of 51.748 kA with a peak current of 128.12 kA. The 33 kV switchboard and generator HV bus show values of 16.60 kA (Ik) and 29.04 kA (Ip). The higher values at the inverter transformer HV side reflect the direct transformation of the 0.4 kV fault current level through the collection of transformers.

At the 132 kV level, the POC_BUS and GT_HV side show a three-phase maximum Ik of 14.09 kA with a peak current Ip of 34.77 kA. The corresponding single-phase maximum values are 35.26 kA (Ik) and 14.29 kA (Ip). The single-phase fault current at 132 kV exceeds the three-phase fault current, which is characteristic of strong transmission networks where the zero-sequence impedance is lower than the positive-sequence impedance, resulting in higher earth fault currents than three-phase fault currents.

The minimum fault current values, calculated with c = 1.0, are consistently lower than the maximum values across all buses. The three-phase minimum at POC_BUS is 12.07 kA (Ik) and 29.78 kA (Ip). These minimum values are used to set the pick-up threshold of overcurrent and distance protection relays, ensuring that the relay can detect the weakest credible fault that would occur under minimum generation conditions.

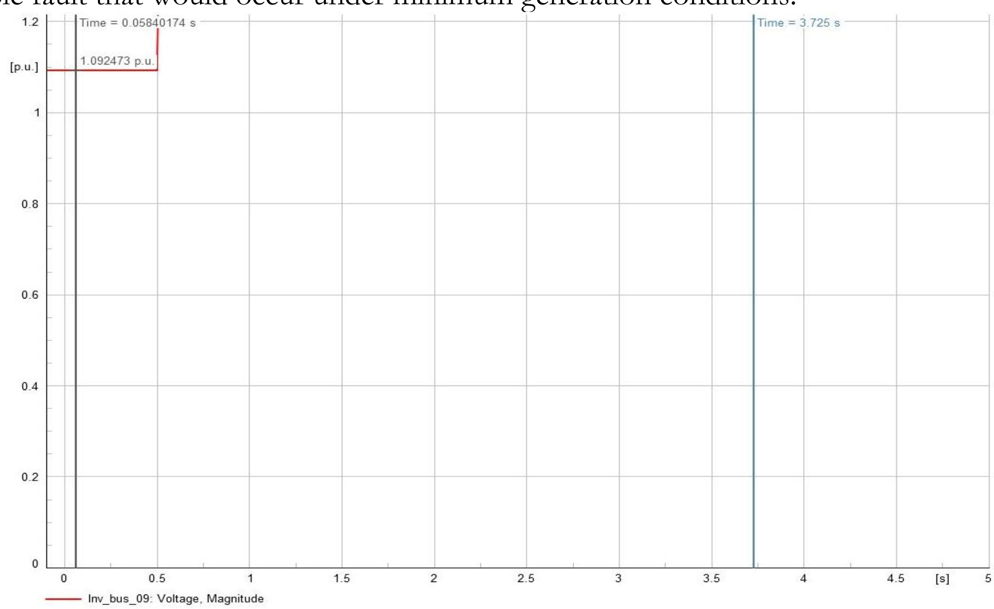

Figure 4. Voltage Magnitude

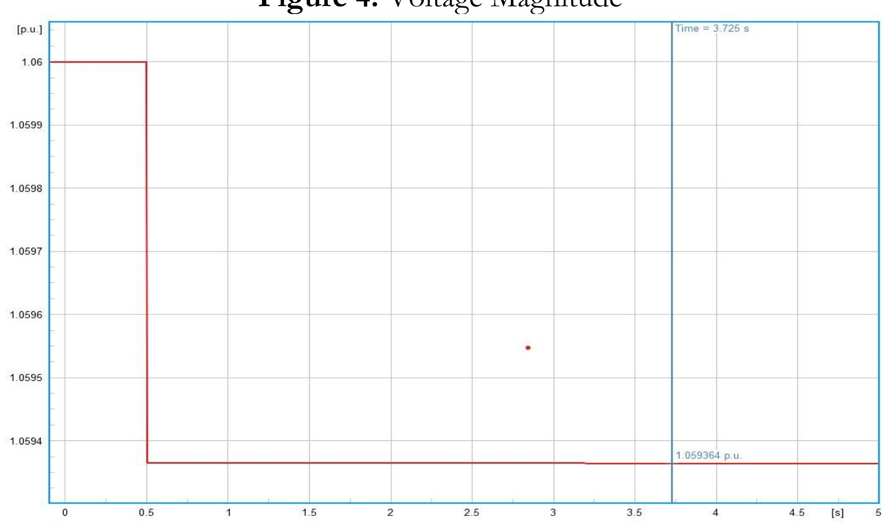

Figure 5. POC_BUS — Voltage Magnitude (p.u.)

The graph shown in Figure 4 presents the voltage magnitude at the inverter bus (Inv_bus_09) over a 5-second simulation window. The y-axis is in per unit (p.u.) with nominal voltage = 1.0 p.u.

A transient overvoltage of about 9.2% of the nominal value occurs during the start-up transient in the inverter bus. After that, a sudden voltage collapse occurs around t = 0.5 s, which suggests that the inverter has tripped or disconnected due to overcurrent/overvoltage protection or a fault condition. The bus continues to be de-energized for the duration of the rest of the simulation, which means that no reconnection takes place during the interval of 5 seconds studied.

The graph shown in Figure 5 represents the voltage magnitude at the Point of Common Coupling (POC) bus, the interface between the local generation system and the utility grid. The y-axis scale is zoomed in between approximately 1.0593 and 1.0601 p.u. to reveal small changes.

The bus voltage response seen in the two graphs directly relates to the generator trip observed at t = 0.5 s, the loss of local generation causes a negligible reduction in bus voltage. The grid is certainly a very stiff one, easily able to absorb the amount of generation loss with no real disturbance. This holds true throughout with the voltage level within tolerances, there is no compliance at the point of common coupling.

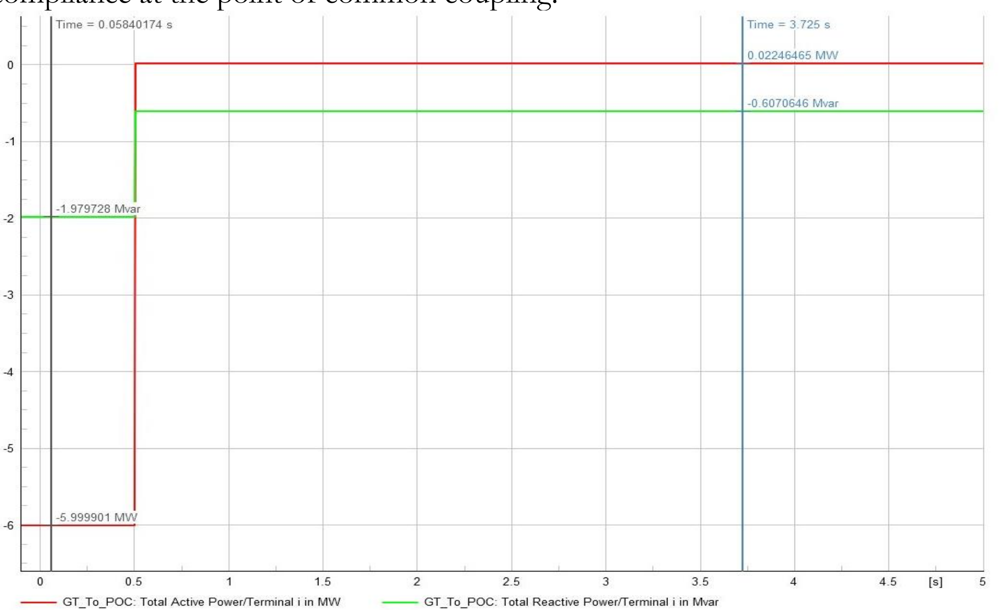

Figure 6. Total Active & Reactive Power (MW / Mvar)

The graph shown in Figure 6 represent the total active power (red trace, MW) and total reactive power (green trace, Mvar) flowing out from the generator/turbine to the POC bus. Negative values show power consumption, instead of power output, from the machine to the grid.

At 0.5 s, a trip occurs, and the active power is dropped to nearly zero, which is an indication of generator disconnection. The small negative active power after the trip, −0.607 Mvar, indicates that there may still be some capacitive load connected to the network, perhaps cable charging or filter capacitors. This behavior is like the complete voltage collapse at Inv_bus_09 seen below.

The graph shown in Figure 7 displays the active power (red trace) and reactive power (green trace) delivered by Inverter 10. The Inverters is always online, and continues to function during the entire simulation, unlike the generator in Graph 3. The active power increases continuously and slowly from around 0.176 MW towards 0.285 MW, typical of a solar PV inverter that is chasing an increasing irradiance profile (e.g., a morning generation ramp).

Reactive power also gradually rises from ~0.047Mvar to ~0.112Mvar, indicating the inverter is providing Reactive power support under a voltage droop or Q(V) control strategy. A smaller increase is seen at t = 0.5 s, which is probably a small compensation response for power sharing when one generator goes out of service, as Inv_10 does.

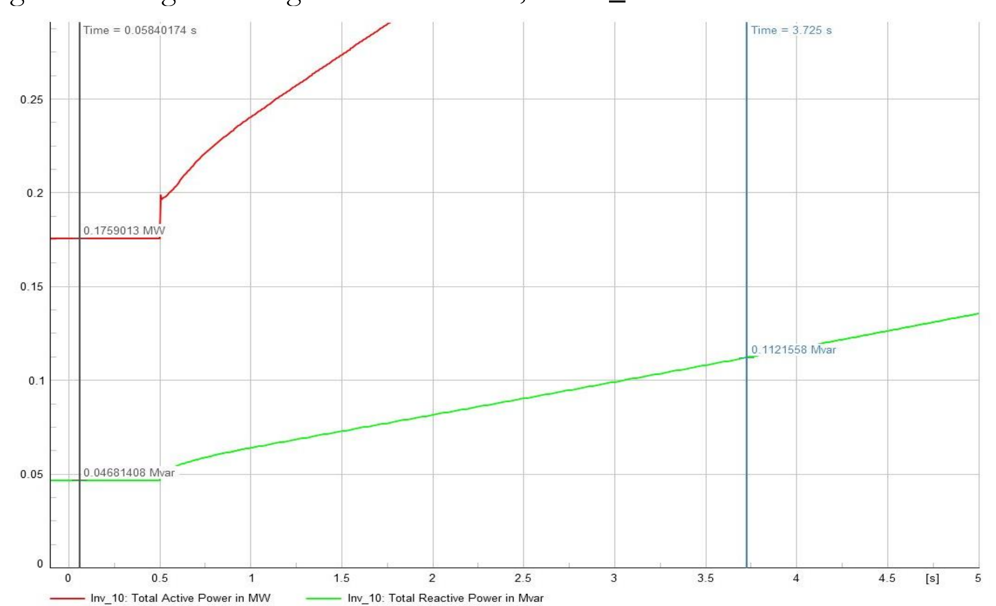

Figure 7. Total Active & Reactive Power (MW / Mvar)

Comparative Analysis with Existing Hybrid Microgrid Studies:

To evaluate the effectiveness of the proposed hybrid renewable microgrid, the obtained simulation results were compared with previously reported hybrid renewable energy systems and microgrid studies available in the literature. Several published studies primarily focused on techno-economic optimization or renewable generation estimation, while limited attention was given to detailed short-circuit behavior, dynamic voltage recovery, and power quality assessment in integrated FPV, hydro, and wind systems.

Compared with previously reported wind–solar hybrid systems [9], the proposed microgrid demonstrated improved voltage stability due to the inclusion of small hydro generation and dynamic reactive power support through the Static Var Compensator (SVC). The hydro generation unit provided stable base-load support, which reduced the impact of renewable intermittency commonly observed in conventional wind–solar systems.

The proposed system also showed improved fault ride-through performance compared with conventional renewable microgrids reported in previous studies [4][13]. During the simulated line-to-line fault event, the voltage at the point of common coupling recovered rapidly to approximately 1.06 p.u. immediately after fault clearance without sustained oscillation or prolonged undervoltage conditions. This behavior indicates improved transient stability and network resilience.

In terms of power quality performance, the proposed system satisfied the Engineering Recommendation P28 limits for voltage fluctuation and flicker severity. Previous studies have reported significant voltage fluctuation problems in renewable-integrated distribution systems under variable solar and wind conditions [13]. However, the incorporation of SVC-based reactive power compensation in the proposed microgrid significantly improved voltage regulation and reduced flicker effects.

The proposed 38-bus hybrid microgrid also provided detailed analysis at multiple voltage levels including 0.4 kV, 11 kV, 33 kV, and 132 kV buses. Unlike many previously published renewable microgrid studies that focused only on energy management or economic optimization, the present work simultaneously evaluated load flow performance, short-circuit current levels, voltage stability, dynamic fault recovery, and power quality compliance within a unified simulation framework.

Furthermore, the integration of floating photovoltaic technology over existing canal water surfaces provided additional operational advantages compared with conventional land-based photovoltaic systems. The FPV system improved land utilization efficiency while benefiting from natural cooling effects, which enhanced renewable generation performance.

Overall, the comparative analysis demonstrates that the proposed FPV–hydro–wind hybrid microgrid offers improved voltage stability, better fault recovery performance, enhanced power quality compliance, and more comprehensive technical evaluation compared with several previously published renewable microgrid studies.

Sensitivity Analysis and System Robustness Evaluation:

To evaluate the robustness and operational reliability of the proposed hybrid renewable microgrid, multiple simulation scenarios and sensitivity analyses were performed under varying operating conditions. The objective of this analysis was to investigate the effect of renewable resource variability, load variation, and fault conditions on voltage stability, power quality, and overall microgrid performance.

Three different renewable generation scenarios were considered during the analysis. In the first scenario, normal operating conditions were simulated using nominal solar irradiance, average wind speed, and standard hydro flow conditions. In the second scenario, reduced solar irradiance and low wind speed conditions were applied to evaluate system performance under unfavorable renewable generation conditions. In the third scenario, increased load demand and severe fault conditions were introduced to assess the dynamic stability and fault ride-through capability of the microgrid.

The sensitivity analysis showed that the proposed hybrid microgrid maintained stable voltage profiles under all simulated operating conditions. Although slight voltage variations were observed during reduced renewable generation scenarios, the bus voltages remained within acceptable operating limits due to the coordinated operation of hydro generation and reactive power support from the Static Var Compensator (SVC).

Under increased load demand conditions, the system experienced a moderate increase in reactive power requirement and network loading. However, the voltage magnitude at the point of common coupling remained close to 1.0 p.u., demonstrating the ability of the proposed hybrid system to maintain operational stability during varying load conditions.

Transient fault simulations further confirmed the robustness of the proposed microgrid. During fault conditions, temporary voltage dips were observed; however, the system demonstrated rapid voltage recovery immediately after fault clearance without sustained oscillations or instability. This indicates strong fault ride-through capability and improved transient performance.

In addition, power quality assessment under varying renewable generation scenarios showed that voltage fluctuation and flicker severity remained within the acceptable limits specified in Engineering Recommendation P28. The inclusion of the SVC significantly reduced voltage fluctuation effects caused by renewable intermittency.

The sensitivity analysis therefore confirms that the proposed FPV–hydro–wind hybrid microgrid can maintain stable and reliable operation under different renewable resource conditions, loading scenarios, and fault disturbances. These results demonstrate the technical robustness and practical applicability of the proposed system for sustainable rural electrification.

Discussion of Voltage Stability, Fault Current, and Power Quality Performance:

The obtained voltage profile results indicate that the proposed hybrid renewable microgrid maintained stable voltage magnitudes across all major buses under normal operating conditions. The voltage magnitude at the point of common coupling remained close to 1.06

p.u., which demonstrates effective voltage regulation and balanced active-reactive power coordination within the network. The relatively stable voltage profile can be attributed to the combined operation of floating photovoltaic, hydro, and wind generation resources together with dynamic reactive power compensation provided by the Static Var Compensator (SVC). The hydro generation unit contributed stable base-load support, while FPV and wind generation supplemented the system according to renewable resource availability.

The voltage profile behavior also demonstrates the ability of the proposed hybrid system to minimize excessive voltage drops commonly observed in renewable-energy-integrated distribution networks. In conventional wind–solar systems, renewable intermittency often causes unstable bus voltages and fluctuating reactive power demand. However, the proposed FPV–hydro–wind configuration improved voltage stability by distributing generation support across multiple renewable resources and voltage levels within the 38-bus network.

The short-circuit analysis results provide important information regarding network strength, equipment rating requirements, and protection coordination. The higher fault current observed at the 33 kV collection buses indicates strong electrical coupling between renewable generation units and the medium-voltage collection network. The maximum three-phase short-circuit current of approximately 14.09 kA at the 132 kV point of common coupling confirms that the proposed system remains within practical transmission-level fault withstand capability limits. Similarly, the lower fault current values observed at the inverter-level buses reflect the limited fault contribution characteristics of inverter-based renewable generation systems.

The transient fault simulations demonstrated strong fault ride-through capability of the proposed microgrid. During the applied fault event, the voltage at the point of common coupling temporarily collapsed; however, the system recovered rapidly after fault clearance without prolonged oscillation or sustained instability. This behavior indicates that the proposed hybrid renewable configuration can maintain synchronization and stable operation during short-duration disturbances. The rapid post-fault voltage recovery also confirms the effectiveness of SVC-based reactive power support in stabilizing network voltage during transient events.

The power quality analysis further demonstrated that the proposed microgrid satisfies the Engineering Recommendation P28 limits for voltage fluctuation and flicker severity. Renewable generation variability, particularly from solar irradiance and wind speed fluctuations, can normally introduce voltage flicker and unstable reactive power behavior. However, the coordinated operation of hydro generation and dynamic reactive power compensation significantly reduced these effects. The observed reduction in voltage fluctuation indicates that the proposed system can provide stable and acceptable power quality for distribution-level consumers.

Overall, the discussion confirms that the proposed FPV–hydro–wind hybrid microgrid provides improved voltage stability, acceptable fault current performance, enhanced transient response, and better power quality behavior compared with conventional renewable-integrated distribution systems. These results demonstrate the technical feasibility and operational reliability of the proposed renewable microgrid for sustainable rural electrification applications.

Practical Implications for Policymakers, Utilities, and Rural Electrification:

The proposed FPV, hydro, wind hybrid renewable microgrid provides several important practical implications for policymakers, electrical utilities, and rural electrification programs in Pakistan and other developing regions facing electricity shortages and unstable grid infrastructure.

From a policymaking perspective, the proposed system demonstrates the technical feasibility of utilizing locally available renewable energy resources for decentralized electricity generation. The integration of floating photovoltaic systems, small hydro generation, and wind energy can support national renewable energy policies aimed at reducing dependence on imported fossil fuels and lowering greenhouse gas emissions. The study also highlights the potential of canal-based floating photovoltaic installations, which can improve land utilization efficiency while simultaneously reducing water evaporation losses. Policymakers can therefore use the proposed framework to support future renewable energy planning and sustainable rural development strategies.

For electrical utilities and distribution network operators, the results demonstrate that hybrid renewable microgrids can improve voltage stability, reduce network loading, and maintain acceptable power quality performance under varying operating conditions. The detailed short-circuit and fault ride-through analyses presented in this work provide useful information for protection coordination, equipment sizing, and grid integration planning. The incorporation of Static Var Compensator (SVC)-based reactive power support further demonstrates how renewable-integrated distribution networks can maintain stable voltage profiles and reduced flicker severity despite renewable intermittency.

The proposed system also has important implications for rural electrification initiatives. Many rural regions in Pakistan continue to experience unreliable electricity supply due to weak transmission infrastructure and insufficient centralized generation capacity. The proposed hybrid microgrid provides a decentralized and sustainable energy solution capable of delivering stable electricity to remote communities using locally available renewable resources. The coordinated operation of floating PV, hydro, and wind generation improves supply continuity and reduces dependence on conventional diesel-based backup systems.

In addition, the proposed hybrid renewable microgrid contributes to environmental sustainability by reducing carbon emissions associated with fossil-fuel-based electricity generation. The use of renewable resources also improves long-term energy security and supports the transition toward cleaner and more resilient power systems.

Overall, the practical findings of this study can support future renewable energy policies, distribution network planning, and rural electrification programs by providing a technically validated hybrid renewable microgrid framework suitable for sustainable energy development in Pakistan and similar developing countries.

Recommendations and Future Perspectives:

Based on the obtained simulation results and technical analysis, several recommendations can be proposed for future deployment, scalability, economic implementation, and policy adoption of the proposed FPV–hydro–wind hybrid renewable microgrid.

First, future deployment of the proposed hybrid microgrid should focus on rural and remote regions with limited access to stable electricity infrastructure. The Takht Bhai case study demonstrates that locally available renewable resources such as canal water flow, solar irradiance, and wind energy can be effectively utilized to develop decentralized and sustainable electricity generation systems. Similar renewable resource assessments can therefore be conducted in other regions of Pakistan to identify suitable locations for hybrid renewable microgrid implementation.

Second, the scalability of the proposed system can be improved through the integration of additional renewable generation units and energy storage technologies. Battery energy storage systems pumped hydro storage, and smart energy management systems can further improve renewable energy utilization, frequency regulation, and supply reliability during fluctuating renewable resource conditions. Future studies may also investigate the integration of electric vehicle charging infrastructure and demand-side energy management within hybrid renewable microgrids.

Third, economic feasibility analysis should be considered in future research to evaluate the lifecycle cost, operational cost, payback period, and financial sustainability of the proposed system. Although the present study primarily focuses on technical analysis, detailed techno-economic optimization would provide valuable information regarding investment planning and large-scale commercial implementation of floating photovoltaic–hydro–wind microgrids.

Fourth, policymakers and government agencies should support the adoption of hybrid renewable microgrids through renewable energy incentives, low-interest financing schemes, and regulatory support for distributed generation systems. National renewable energy policies should encourage floating photovoltaic installations over existing canal and reservoir systems to improve land utilization efficiency and renewable energy capacity expansion.

Furthermore, electrical utilities and distribution network operators should consider hybrid renewable microgrids as a long-term solution for improving rural electrification, reducing transmission losses, and minimizing dependence on conventional fossil-fuel-based generation. The inclusion of reactive power compensation devices and modern microgrid control strategies can also support stable grid integration of renewable resources.

Finally, future research may extend the present work by incorporating real-time hardware implementation, advanced optimization algorithms, artificial intelligence-based energy management systems, and cybersecurity analysis for smart renewable microgrids. These developments can further enhance the reliability, operational efficiency, and practical applicability of renewable-energy-based decentralized power systems.

Conclusion:

A hybrid microgrid based on Floating Solar PV, Small Hydro, and Wind power sources was successfully designed for the Takht Bhai area in Mardan. The primary goal was to use renewable resources available in the region to design a reliable power generation system without compromising power quality. The entire system was modelled and analysed in DIgSILENT PowerFactory using a 38-bus network. The simulation results indicated that the proposed system operated well across various operating conditions. The load flow analysis verified that the bus voltages remained within the acceptable range, indicating the system would operate well. Short-circuit and fault analysis also revealed that the system effectively withstands disturbances, and after the fault is cleared, the voltage quickly recovers to its normal value. Furthermore, the power quality evaluation under the P28 standard showed that voltage fluctuations and flicker were within acceptable limits. The integration of hydro, floating PV, and wind generation reduced the disadvantages, creating a more predictable and secure electricity supply. In the future, implementing closed-loop control to regulate voltage, frequency, and power flow in real time will improve system stability and dynamic performance.

References:

[1] M. A. Sheikh, “Energy and renewable energy scenario of Pakistan,” *Renew. Sustain. Energy Rev.*, vol. 14, no. 1, pp. 354–363, 2010, doi: https://doi.org/10.1016/j.rser.2009.07.037.

[2] Moslem Uddin, Huadong Mo, “Microgrids: A review, outstanding issues and future trends,” *Energy Strateg. Rev.*, vol. 49, 2023, [Online]. Available: https://www.sciencedirect.com/science/article/pii/S2211467X23000779

[3] Majid Ali, Mohsin Riaz, Mohsin Ali Koondhar, Muhammad Sarfraz Akram, “Renewable energy sources-based hybrid microgrid system for off-grid electricity solution for rural communities,” *Energy Sci. Eng.*, 2023, [Online]. Available: https://scijournals.onlinelibrary.wiley.com/doi/10.1002/ese3.1535

[4] Nathan Lee, Ursula Grunwald, “Hybrid floating solar photovoltaics-hydropower systems: Benefits and global assessment of technical potential,” *Renew. Energy*, vol.

162, pp. 1415–1427, 2020, doi: https://doi.org/10.1016/j.renene.2020.08.080.
[5] Evgeny Solomin, Evgeny Sirotkin, "Hybrid Floating Solar Plant Designs: A Review," *Energies*, vol. 14, no. 10, p. 2751, 2021, doi: https://doi.org/10.3390/en14102751.
[6] Laura Essak, Aritra Ghosh, "Floating Photovoltaics: A Review," *Clean Technol*, vol. 4, no. 3, pp. 752–769, 2022, doi: https://doi.org/10.3390/cleantechnol4030046.
[7] Zeyu Ding, Hongjuan Hou, "Performance analysis of a wind-solar hybrid power generation system," *Energy Convers. Manag.*, vol. 181, pp. 223–234, 2019, doi: https://doi.org/10.1016/j.enconman.2018.11.080.
[8] M. Farrokhabadi *et al.*, "Microgrid Stability Definitions, Analysis, and Examples," *IEEE Trans. Power Syst.*, vol. 35, no. 1, pp. 13–29, Jan. 2020, doi: 10.1109/TPWRS.2019.2925703.
[9] M. Faisal, M. A. Hannan, P. J. Ker, A. Hussain, M. B. Mansor and F. Blaabjerg, "Review of Energy Storage System Technologies in Microgrid Applications: Issues and Challenges," *IEEE Access*, vol. 6, pp. 35143–35164, 2018, doi: 10.1109/ACCESS.2018.2841407.
[10] J. Rocabert, A. Luna, F. Blaabjerg, and P. Rodríguez, "Control of power converters in AC microgrids," *IEEE Trans. Power Electron.*, vol. 27, no. 11, pp. 4734–4749, 2012, doi: 10.1109/TPEL.2012.2199334.
[11] Lauren E. Natividad, Pablo Benalcazar, "Hybrid Renewable Energy Systems for Sustainable Rural Development: Perspectives and Challenges in Energy Systems Modeling," *Energies*, vol. 16, no. 3, p. 1328, 2023, doi: https://doi.org/10.3390/en16031328.
[12] Regina Lamedica, Ezio Santini, "A MILP methodology to optimize sizing of PV - Wind renewable energy systems," *Energy*, vol. 165, pp. 385–398, 2018, doi: https://doi.org/10.1016/j.energy.2018.09.087.
[13] "(PDF) A Review on Floating Photovoltaic Technology (FPVT)." Accessed: Jun. 16, 2026. [Online]. Available: https://www.researchgate.net/publication/355251818_A_Review_on_Floating_Photovoltaic_Technology_FPVT
[14] Yujun Li, Zhao Xu, "A cascading power sharing control for microgrid embedded with wind and solar generation," *Renew. Energy*, vol. 132, pp. 846–860, 2019, doi: https://doi.org/10.1016/j.renene.2018.07.150.
[15] F. Blaabjerg, Y. Yang, D. Yang and X. Wang, "Distributed Power-Generation Systems and Protection," *Proc. IEEE*, vol. 105, no. 7, pp. 1311–1331, 2017, doi: 10.1109/JPROC.2017.2696878.
[16] M. H. Rehmani, M. Reisslein, A. Rachedi, M. Erol-Kantarci, and M. Radenkovic, "Integrating Renewable Energy Resources into the Smart Grid: Recent Developments in Information and Communication Technologies," *IEEE Trans. Ind. Informatics*, vol. 14, no. 7, pp. 2814–2825, Jul. 2018, doi: 10.1109/TII.2018.2819169.
[17] J. M. Guerrero, J. C. Vasquez, J. Matas, L. G. De Vicuña, and M. Castilla, "Hierarchical control of droop-controlled AC and DC microgrids - A general approach toward standardization," *IEEE Trans. Ind. Electron.*, vol. 58, no. 1, pp. 158–172, Jan. 2011, doi: 10.1109/TIE.2010.2066534.
[18] Hassan Bevrani, Toshifumi Ise, "Virtual synchronous generators: A survey and new perspectives," *Int. J. Electr. Power Energy Syst.*, vol. 54, pp. 244–254, 2014, [Online]. Available: https://www.sciencedirect.com/science/article/pii/S0142061513003062
[19] M. V. Karthik and P. Chaudhary, "Power Quality Enhancement in AC Microgrids Using Integrated Genetic Algorithm in ANN," *Proc. 5th Int. Conf. Electron. Commun. Aerosp. Technol. ICECA 2021*, pp. 237–244, 2021, doi: 10.1109/ICECA52323.2021.9675866.

[20] Salman Hajiaghasi, Ahmad Salemnia, "Hybrid energy storage system for microgrids applications: A review," *J. Energy Storage*, vol. 21, pp. 543–570, 2019, doi: https://doi.org/10.1016/j.est.2018.12.017.
[21] FH Applications, Marco Marengo, "Applications of Energy Storage Systems in Enhancing Energy Management and Access in Microgrids: A Review," *Energies*, vol. 16, no. 16, p. 5930, 2023, doi: https://doi.org/10.3390/en16165930.
[22] Subhojit Dawn, A. Ramakrishna, M. Ramesh, Shreya Shree Das, K. Dhananjay Rao, "Integration of Renewable Energy in Microgrids and Smart Grids in Deregulated Power Systems: A Comparative Exploration," *Adv. Energy Sustain. Res.*, 2024, [Online]. Available: https://advanced.onlinelibrary.wiley.com/doi/10.1002/aesr.202400088
[23] Binayak Bhandari, Kyung-Tae Lee, Gil-Yong Lee, Young-Man Cho & Sung-Hoon Ahn, "Optimization of hybrid renewable energy power systems: A review," *Int. J. Precis. Eng. Manuf. Technol.*, vol. 2, pp. 99–112, 2015, [Online]. Available: https://link.springer.com/article/10.1007/s40684-015-0013-z
[24] "(PDF) DESIGN AND OPTIMIZATION OF HYBRID RENEWABLE ENERGY SYSTEM FOR RURAL ELECTRIFICATION OF AN OFF-GRID COMMUNITY." Accessed: Jun. 15, 2026. [Online]. Available: https://www.researchgate.net/publication/370845571_DESIGN_AND_OPTIMIZATION_OF_HYBRID_RENEWABLE_ENERGY_SYSTEM_FOR_RURAL_ELECTRIFICATION_OF_AN_OFF-GRID_COMMUNITY
[25] M. Kamran *et al.*, "Reconsidering the power structure of Pakistan," *Int. J. Renew. Energy Res.*, vol. 9, no. 1, pp. 480–492, Mar. 2019, doi: 10.20508/IJRER.V9I1.8954.G7606.
[26] "Power system stability and control | Semantic Scholar." Accessed: Jun. 15, 2026. [Online]. Available: https://www.semanticscholar.org/paper/Power-system-stability-and-control-Kundur/1c2040faf07594e60bd7dd339cf363a867416ef8